Synthesis, structural characterisation and bonding in an anionic hexavanadate bearing redox-active ferrocenyl groups at the periphery†

Jiří Schulz,[a] Róbert Gyepes,[ab] Ivana Císařová[a] and Petr Štěpnička*[a]

Received (in Victoria, Australia) 2nd June 2010, Accepted 18th July 2010
DOI: 10.1039/c0nj00421a

Amide $FcCONHC(CH_2OH)_3$ (**1**; Fc = ferrocenyl), prepared from fluorocarbonylferrocene and tris(hydroxymethyl)methylamine, reacts with $(Bu_4N)_3[H_3V_{10}O_{28}]$ in *N*,*N*-dimethylacetamide to afford a salt containing a bis(triolato) capped hexavanadate anion bearing two ferrocenyl groups at its periphery, $(Bu_4N)_2[\{FcC(O)NHC(CH_2O)_3\}_2V_6O_{13}]$ (**2**). Compounds **1** and **2** were characterised by elemental analysis, spectroscopic methods (IR, NMR, and MS) and by cyclic voltammetry; the crystal structures of $\mathbf{1}\cdot 1/2CH_3CO_2Et$ and $(Bu_4N)_2[\{FcC(O)NHC(CH_2O)_3\}_2V_6O_{13}]\cdot 2Me_2NCHO$ were determined by X-ray diffraction analysis. Single-point DFT calculations performed for the isolated hexavanadate anion revealed the presence of 3-centre 4-electron (3c4e) O–V–O bonds on the hexavanadate cage, which are responsible for the high energy of the occupied frontier orbitals. The upper eleven occupied molecular orbitals including the HOMO are all delocalized over the hexavanadate cage and, therefore, any electrochemical oxidation can be expected to occur preferentially at the hexavanadate anion without affecting the pendant ferrocene moieties.

Introduction

Early transition metal polyoxoanions, commonly called polyoxometalates,[1] have been studied originally as structurally attractive and synthetically challenging compounds. More recently, the interest in these compounds renewed, being stimulated by attempts to find new cluster types and large cages mimicking the properties of metal oxides. Further motivation comes from the applications of polyoxometalates and their derivatives in a broad range of fields ranging from material science and catalysis to biology and biomedicine.[2]

Hexavanadate clusters are no exception and a number of compounds having the parent hexavanadate core modified *via* incorporation of late transition metal organometallic units[3] or a (formal) replacement of the bridging oxygen atoms with alkoxo groups[4] have been reported. Compounds in which triolate units replace the bridging oxygen atoms at the open tetrahedral cavities of the parent $\{V_6O_{19}\}$ core are particularly attractive due to their synthetic accessibility.[5] For instance, the bis-capped anions $[V_6O_{13}\{(OCH_2)_3CR\}]^{2-}$ can be prepared *via* condensation of $[H_3V_{10}O_{28}]^{3-}$ with triols $(HOCH_2)_3C–R$[5a] with a range of functional groups at the periphery (variation of R).[5c,6] The practical potential of such materials was already demonstrated by the preparation of coordination networks showing catalytic activity in oxidation reactions.[6]

Aiming at the preparation of hitherto unknown ferrocenyl-modified polyvanadates, we utilised the mentioned synthetic approach using *N*-{[tris(hydroxymethyl)methyl]carbamoyl}-ferrocene as a source of the ferrocenyl (Fc) unit. Herein, we describe the synthesis of a novel hexavanadate bearing two amidoferrocene pendants and its structural characterisation *via* a combination of spectroscopic methods, X-ray diffraction analysis, cyclic voltammetry and DFT calculations.

Results and discussion

Syntheses and structural characterisation

The starting triol derivative, $FcCONHC(CH_2OH)_3$ (**1**), was prepared (Scheme 1) by reacting fluorocarbonylferrocene with tris(hydroxymethyl)methylamine in the presence of 4-(dimethylamino)pyridine and triethylamine using dry *N*,*N*-dimethylformamide (DMF) as a solvent. Isolation by column chromatography followed by crystallisation from ethyl acetate–hexane afforded an unstable solvate $\mathbf{1}\cdot 1/2CH_3CO_2Et$ (**1a**). Upon drying under vacuum, this adduct partly liberated the solvent of crystallisation being converted to a non-stoichiometric though somewhat more stable solvate analysed as $\mathbf{1}\cdot 1/3CH_3CO_2Et$ (**1b**), which was used in the subsequent reactions.

Compound **1b** was characterised by elemental analysis and by spectroscopic methods. In its IR spectrum, it displays diagnostic amide bands[7] at 1619 and 1535 cm^{-1}, and a carbonyl stretching band of the solvating ethyl acetate at 1740 cm^{-1}. The NMR spectra of **1b** show signals attributable to the ferrocenyl moiety and the amide pendant. The amide C=O signal is seen at δ_C 170.10, similarly to an analogous 2-hydroxyethyl substituted amide, $FcCONHCH_2CH_2OH$.[8]

[a] *Department of Inorganic Chemistry, Faculty of Science, Charles University in Prague, Hlavova 2030, 12840 Prague, Czech Republic. E-mail: stepnic@natur.cuni.cz; Fax: +420 221 951 253*
[b] *J. Heyrovský Institute of Physical Chemistry, Academy of Sciences of the Czech Republic, v.v.i., Dolejškova 3, 18223 Prague 8, Czech Republic*

† Electronic supplementary information (ESI) available: A 'full view' of the crystal structure of **2a**, a superposition of the two crystallographically independent anions in the structure of **2a**, and the crystallographic data for **1a** and **2a**. CCDC reference numbers 779152 and 779153. For crystallographic data in CIF or other electronic format see DOI: 10.1039/c0nj00421a

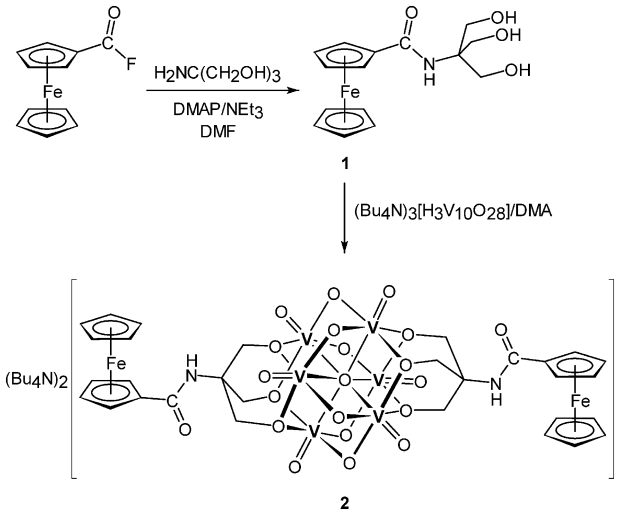

Scheme 1 The synthesis of **1** and **2** (DMAP = 4-(dimethylamino)-pyridine, DMA = *N*,*N*-dimethylacetamide, DMF = *N*,*N*-dimethyl formamide).

The molecular structure of **1a** as determined by X-ray crystallography (Fig. 1) is rather unexceptional. The ferrocene unit possessed a regular geometry, showing negligible tilting of its cyclopentadienyl rings (dihedral angle being only 1.2(1)°) and variation in the individual Fe–C(ring) distances (2.032(1)–2.055(2) Å). The distances of the iron atom to the cyclopentadienyl ring centroids are 1.6465(8) and 1.6505(9) Å for the substituted and unsubstituted rings, respectively. The geometry of the amide group does not differ much from that of the mentioned 2-hydroxyethyl amide,[8] or the non-functional amides FcCONHR, where R = *i*-Pr,[9] *n*-Bu, C_6H_{11}, Ph,[10] and CH_2Ph.[11]

In the crystal, the molecules of the amide associate *via* conventional O–H···O hydrogen bonds (Fig. 2). The molecular array can be described such that the molecules related by the crystallographic two-fold axes assemble into pairs by O4–H4O···O3 contacts, whilst the dimers formed aggregate

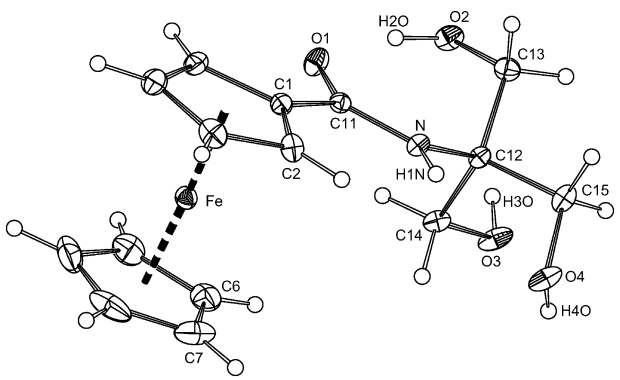

Fig. 1 PLATON[12] plot of the amide molecule in the structure of **1a** showing the atom labelling and displacement ellipsoids at the 30% probability level. Selected distances and angles (in Å and °): C1–C11 1.477(2), C11–O1 1.244(2), C11–N 1.343(2), N–C12 1.474(2), C12–C13 1.544(2), C12–C14 1.534(2), C12–C15 1.530(2), C13–O2 1.416(2), C14–O3 1.423(2), C15–O4 1.426(2); O1–C11–N 122.8(1), C11–N–C12 124.4(1), N–C12–C(13/14/15) 106.6(1)–112.8(1), C12–C(13/14/15)–O(2/3/4) 110.8(1)–115.2(1).

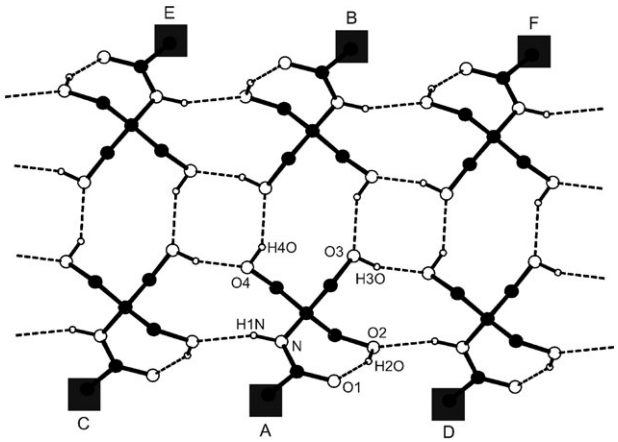

Fig. 2 A section of the hydrogen bonded array in the structure of **1a** as viewed along the crystallographic *b* axis. For clarity, the ferrocenyl units have been replaced with filled black squares. Hydrogen bond parameters are as follows: N–H1N···$O2^C$, N···$O2^C$ = 3.076(2) Å, angle at H1N = 148°; O2–H2O···O1, O2···O1 = 2.649(2) Å, angle at H2O = 152°; O3–H3O···$O4^D$, O3···$O4^D$ = 2.663(2) Å, angle at H3O = 164°; O4–H4O···$O3^B$, O4···$O3^B$ = 2.671(2) Å, angle at H4O = 147°. Symmetry operations: *A* = (*x*, *y*, *z*), *B* = (−*x*, *y*, 1/2 − *z*), *C* = (*x*, 1 − *y*, −1/2 + *z*), *D* = (*x*, 1 − *y*, 1/2 + *z*), *E* = (−*x*, 1 − *y*, −*z*), *F* = (−*x*, 1 − *y*, 1 − *z*).

further into infinite ribbons oriented parallel to the *ac* plane by means of the O3–H3O···O4 and N–H1N···O2 lateral hydrogen bonds. Besides, the mutual orientation of the polar groups allows for the formation of structure-stabilising intramolecular O2–H2O···O1 contacts.[13] Molecules of the solvent occupy structural voids defined by the relatively bulkier amide molecules and do not interact apparently with the mentioned molecular assembly.

When reacted with $(Bu_4N)_3[H_3V_{10}O_{28}]$ in dry *N*,*N*-dimethylacetamide (DMA) at elevated temperatures, amide **1** behaved similarly to other tris(hydroxymethyl)methyl derivatives, affording the respective cationic hexavanadate, $(Bu_4N)_2[FcC(O)NHC(CH_2O)_3V_6O_{13}(OCH_2)_3CNHC(O)Fc]$ (**2**; Scheme 1). Compound **2** could be conveniently isolated by column chromatography (silica gel/MeCN). However, a better defined, air-stable red crystalline solvate **2**·2Me_2NCHO (**2a**) resulted *via* a subsequent crystallisation from a MeCN–DMF–diethyl ether mixture (15% isolated yield of analytically pure product after chromatography and two crystallisations).

The formulation of **2a** is consistent with elemental analysis data and also with electrospray mass spectra indicating the presence of the ionic constituents through the signals due to Bu_4N^+ (*m*/*z* 242), $[\{FcCONHC(CH_2O)_3\}_2V_6O_{13}]^{2-}$ (*m*/*z* 587), and $[\{FcCONHC(CH_2O)_3\}_2V_6O_{13} + Na]^-$ (*m*/*z* 1197). The IR spectra of **2a** suggest the presence of the vanadate unit and carbonyl groups. A very strong $\nu_{V=O}$ band is seen at 952 cm^{-1}. Amide bands attributable to the amidoferrocene pendants appear at 1655/1652 and 1536/1533 cm^{-1}. Notably, the former band, largely $\nu_{C=O}$ (amide I), is shifted to higher energies as compared to **1b**, reflecting the differences in hydrogen bonding patterns. On the other hand, the other (amide II, δ_{NH}) band remains virtually unaffected. An additional $\nu_{C=O}$ band due to solvating DMF occurs at 1674 cm^{-1}.

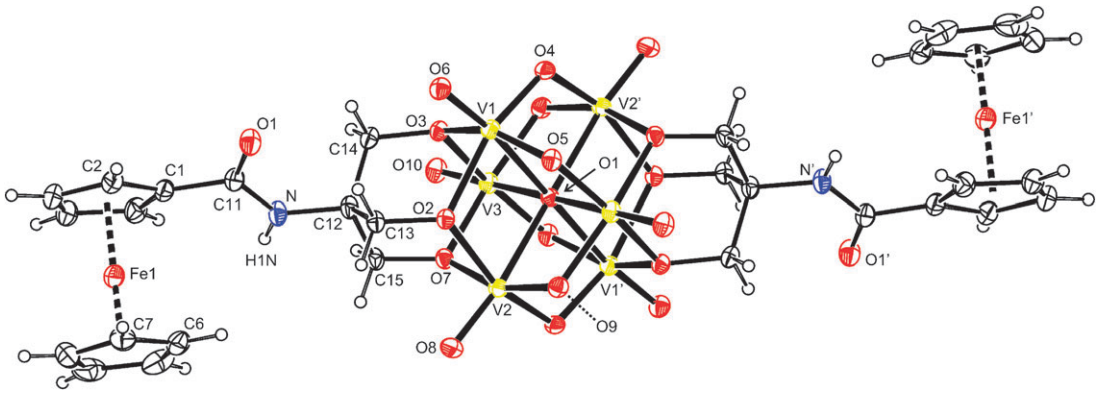

Fig. 3 PLATON[12] plot of anion 1 in the structure of **2a** showing displacement ellipsoids with 30% probability. The primed atoms are generated by the crystallographic inversion. The structure and atom labelling scheme of anion 2 in the structure of **2a** are essentially identical. Atomic labels in anion 2 are obtained by adding 20 to the respective label in anion 1.

The ^{51}V NMR spectrum of **2a** recorded in CD_3CN exhibits a single broad resonance at δ_V −498. The ^{1}H and ^{13}C NMR spectra confirm the presence of the amidoferrocene pendant, the counterions and the solvating DMF. Whereas the resonances of the FcC(O) moiety remain virtually intact upon 'complexation' (*cf.* δ_C(C═O) 170.90), those due to the $C(CH_2O)_3$ are affected significantly. The signals of the CH_2O groups are shifted to lower fields in both the ^{1}H and ^{13}C NMR spectra ($\Delta\delta_H \approx 1.7$ ppm, $\Delta\delta_C \approx 23$ ppm), and the C-13 resonance of the $C(CH_2O)_3$ carbon moves by *ca.* 8 ppm upfield (*N.B.* the spectra of **1b** and **2a** were recorded in different solvents).

The solid-state structure of **2a** was determined by single-crystal X-ray diffraction analysis (Fig. 3 and Table 1). It

Table 1 Selected distances and angles for the hexavanadate anions in the structure of **2a** (in Å and °)[a]

Anion 1		Anion 2	
V1–O1 (c)	2.2491(5)	V21–O21 (c)	2.2362(5)
V1–O2 (a)	2.057(2)	V21–O22 (a)	2.046(2)
V1–O3 (a)	1.983(2)	V21–O23 (a)	1.991(2)
V1–O4 (b)	1.771(2)	V21–O24 (b)	1.779(2)
V1–O5 (b)	1.886(2)	V21–O25 (b)	1.876(2)
V1–O6 (t)	1.603(2)	V21–O26 (t)	1.605(2)
V2–O1 (c)	2.2276(5)	V22–O21 (c)	2.2320(4)
V2–O2 (a)	1.982(2)	V22–O22 (a)	1.992(2)
V2–O7 (a)	2.064(2)	V22–O27 (a)	2.063(2)
V2–O4′ (b)	1.887(2)	V22–O24′ (b)	1.864(2)
V2–O9 (b)	1.761(2)	V22–O29 (b)	1.773(2)
V2–O8 (t)	1.605(2)	V22–O28 (t)	1.611(2)
V3–O1 (c)	2.2439(5)	V23–O21 (c)	2.2594(5)
V3–O3 (a)	2.062(2)	V23–O23 (a)	2.052(2)
V3–O7 (a)	1.975(2)	V23–O27 (a)	1.989(2)
V3–O9′ (b)	1.886(2)	V23–O29′ (b)	1.882(2)
V3–O5′ (b)	1.761(2)	V23–O25′ (b)	1.777(2)
V3–O10 (t)	1.605(2)	V23–O30 (t)	1.603(2)
V–O(a)–V	109.23(8)–110.05(8)		109.02(8)–110.13(8)
O(c)–V–O(t)	171.88(8)–171.89(8)		172.66(7)–172.76(7)
Fe1–Cg1	1.650(2)	Fe21–Cg21	1.650(2)
Fe1–Cg2	1.654(2)	Fe21–Cg22	1.651(2)
∠Cp1,Cp2	2.0(2)	∠Cp21,Cp22	1.8(2)
C11–O11	1.227(4)	C31–O31	1.232(4)
C11–N1	1.349(4)	C31–N21	1.352(4)
O11–C11–N1	123.9(3)	O31–C31–N21	123.8(3)
N1–C12	1.470(4)	N21–C32	1.476(4)
C12–C13	1.541(4)	C32–C33	1.532(4)
C13–O2	1.431(3)	C33–O22	1.424(3)
C12–C14	1.537(4)	C32–C34	1.535(4)
C14–O3	1.428(3)	C34–O23	1.434(3)
C12–C15	1.534(4)	C32–C35	1.541(4)
C15–O7	1.421(3)	C35–O27	1.429(3)
V–O(a)–C	117.4(2)–120.2(2)		117.9(2)–120.0(2)

[a] For atom labelling scheme, see Fig. 1. The prime-labelled atoms are generated by inversion operations. Definitions: a = alcoholate oxygen atom (O2, O3, and O7), b = bridging oxido ligands (O4, O5, O9), c = central oxygen atom (O1), t = terminal oxido ligands (O6, O8, O10). Cp1 and Cp2 are the substituted and unsubstituted cyclopentadienyl rings, respectively. Cg1 and Cg2 stand for their respective centroids.

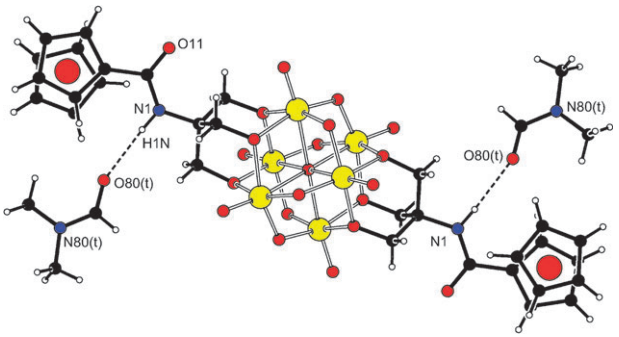

Fig. 4 Hydrogen bonds formed between cation 1 and the solvating DMF in the structure of **2a**. The hydrogen bonding pattern generated by cation 2 is similar. Hydrogen bond parameters: cation 1, N1–H1N···O80, N1···O80 = 3.114(4) Å, angle at H1N = 175°; cation 2, N21–H21N···O90, N21···O90 = 3.042(4) Å, angle at H21N = 167°; t = molecules generated by lattice translations.

consists of discrete Bu_4N^+ ions and hexavanadate anions, which bind two DMF molecules *via* FcCO*N*–*H*···*OC*(H)NMe$_2$ hydrogen bonds (Fig. 4). Notably, there are two structurally independent albeit practically identical[14] hexavanadate ions in the crystal structure, each residing on the crystallographic inversion centres (for an overlap and a 'full view', see ESI†). As a result, the asymmetric unit contains two Bu_4N^+ cations, two halves of the hexavanadate anions and two molecules of solvating DMF.

The triolate units in the anion of **2a** are mutually *trans* as dictated by the imposed symmetry and the overall geometry compares well with that reported for the structurally related anions $[\{RC(CH_2O)_3\}_2V_6O_{13}]^{2-}$, where R = NO_2,[5a] CH_3,[5c,d] NHC(O)CH=CH_2,[5c] or CH_2OH.[5g] Likewise these reference compounds, the V–O distances in **2a** follow the trend: V–O(terminal) < V–O(oxo bridge) < V–O(alkoxide bridge) < V–O1 (central oxygen), which in turn leads to an alternation of the V–O distances within the three V_4O_4 rings encircling the central oxygen atom O1.

The geometry of the V_6O (O = O1) core is quite regular, only with the V2–O1 distance being slightly longer than those involving vanadium atoms V2 and V3. The in-cage V–O1–V angles amount either to *ca.* 95° or *ca.* 85°, accordingly as the respective vanadium atoms belong to an alkoxide- or oxide-bridged edge of the V_6 octahedron. Another deformation is detected at the outer surface of the hexavanadate core because the terminal oxygen atoms, O(6,8,10), are all displaced from the respective O1–V axes and moved away from the closest triol-capped face. Nevertheless, this deformation is relatively minor (*cf.* the O1–V–O(t) angles being *ca.* 171.9° [172.7°])[15] and very likely reflects steric interactions of the terminal V=O groups with the CH_2O arms.

Despite these distortions and unlike V–O distances, the oxygen atoms forming the 'central layer', *viz.* O1, O(7/7′), O(8,8′), O(9,9′) and O(10,10′), are coplanar within *ca.* 0.06 Å [0.04 Å], whilst the V2 and V3 atoms deviate from this central plane by 0.044(1) Å and 0.132(1) Å [0.058(1) and 0.124(1) Å], respectively. The oxygen atoms constituting 'equatorial' O_4 planes, which are roughly perpendicular to the O=V–O1 axes (*i.e.*, O(2–5) for V1, O(2,7,9,4′) for V2, and O(3,7,5′,9′) for V3), are coplanar within less than 0.01 Å. However, their 'central' vanadium atoms, V(1–3), are displaced from these planes away from the central oxygen O1. The distances from the respective mean O_4-planes are 0.356(1) Å [0.348(1) Å] for V1, 0.337(1) Å [0.341(1) Å] for V2, and 0.350(1) Å [0.363(1) Å] for V3. The O(2–5) plane is almost coplanar with the central plane (the dihedral angle being 0.49(6)° [0.48(6)°]), whereas the remaining two O_4-planes are oriented perpendicularly (the dihedral angles are 89.71(6)° [89.86(6)°] for O(2,7,9,4′), and 89.65(6)° [89.59(6)°] for O(3,7,5′,9′)).

The arms of the triolato unit constitute three OVOCCC metallorings, which assume similar chair conformations and bear the pivotal N–C(O) bond in equatorial positions. Structural parameters of the ferrocenyl pendant differ only marginally from those of **1a**. The ferrocene cyclopentadienyls in **2a** are negligibly tilted and bind symmetrically to the iron atom. Notably, the amide planes {CON} are rotated with respect to their bonding cyclopentadienyl ring by 25.9(4)° [23.6(4)°], with the oxygen atom being moved away from the ferrocene core. On the other hand, changes in the arrangement of the amide moiety as well as the variation in the C–CH_2O and CCH_2–O bond lengths are rather insignificant. All other parameters (including those of the Bu_4N^+ cations and the solvating DMF)[16] are unexceptional.

Electrochemistry

Compounds **1b** and **2a** were studied by cyclic voltammetry at Pt-disc electrode using *ca.* 5×10^{-4} M acetonitrile solutions containing 0.1 M Bu_4NPF_6 as the supporting electrolyte. The amide expectedly showed a single, one-electron reversible wave attributable to ferrocene/ferrocenium couple. This wave was observed at more positive potentials than for ferrocene itself ($E^{\circ\prime}$ = 0.20 V), which is, indeed, in accordance with the electron-withdrawing nature of the carbamoyl unit (*cf.* σ_P = 0.36 for $CONH_2$).[17]

Compound **2a** also displayed a single oxidative wave in the potential window provided by the solvent (Fig. 5). However, this wave was found to be electrochemically irreversible (anodic peak potential, E_{pa} = +0.12 V at the scan rate of 100 mV s^{-1}; no reduction counter-peak was seen up to 10 V s^{-1}).

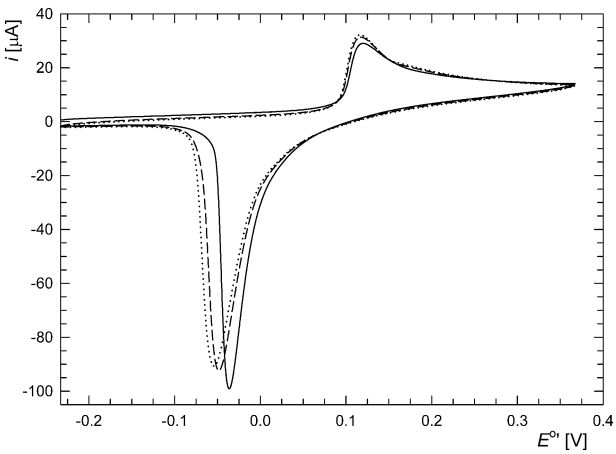

Fig. 5 Cyclic voltammogram of **2a** as recorded on a Pt-disc electrode in MeCN (c = 0.5 mM in 0.1 M Bu_4NPF_6). The first scan (full line) and the following scans are distinguished by the line type (second scan in dashed line, third in dotted line).

Moreover, a stripping-like peak (probably desorption) developed upon back scanning which shifted to slightly less positive potentials during the following scans (Fig. 5). This indicates some structural changes to be associated with the primary electron-transfer process that makes the redox change electrochemically (and also chemically) irreversible.

Notably, no reduction peak was seen for **2a** down to −2.4 V *vs.* the ferrocene/ferrocenium reference. This contrasts with the behaviour of $[\{RC(CH_2O)_3\}_2V_6O_{13}]^{2-}$, where R = CH_3, CH_2CH_3, CH_2Ph, NO_2, and NMe_2, that all display one-electron reversible *reductions* in the potential range of *ca.* −0.65 to −1.2 V (*vs.* ferrocene/ferrocenium) depending on R.[5a,d] An explanation of the overall redox response of **2a** can be sought in the electron-donating character of the ferrocenyl group, which makes the hexavanadate unit (relatively) electron rich and thus renders any reduction more difficult while facilitating oxidation processes.

DFT calculations

The solid state structure of the anion in **2** has been subjected to single-point DFT studies in order to obtain some insight into the bonding relations within the hexavanadate unit.

The peculiar structure of the hexavanadate cage owes its existence to a rather complicated bonding scheme, which is impossible to describe properly by the 'classical' Lewis terms (*i.e.*, *via* σ- and π-bonds between atoms and nonbonding electron lone pairs). Although the natural charges of the individual vanadium atoms were found to be practically the same (1.54 for V1/1′ and V3/3′; 1.53 for V2/2′), those of the hexavanadate oxygen atoms exhibited a large variation depending on the number of the bonding partners (Table 2). In addition, the Mayer bond orders[18] were dependent on the chemical nature of the individual oxygen atoms (Table 3), while the fractional values obtained for the V–O bonds suggested that only a resonance description of the bonding could be adequate.

The nearly regular octahedron around the central oxygen atom O1 cannot be the result of any dominant O–V covalent interactions, since an octahedral arrangement is achievable by the formation of a sp^3d^2 hybrid, which is however beyond the possibilities of the second-row oxygen atom. The primary role of the O1 atom is thus to act as an 'anchor' for the surrounding vanadium cations by means of its marked negative charge, alleviating the repulsion between the metallic centres and providing some necessary electrostatic stabilization for the hexavanadate cage.

Owing to their octahedral environment, the O1 2s and 2p orbitals remain unmixed and despite being virtually nonbonding, they still provide some covalent bonding contributions to the surrounding metallic centres. However, due to the large interatomic O1–V separations, these covalent contributions are rather weak; thus the Natural Bond Orbital[19] (NBO) default search reported four lone pairs on O1 with the covalent overlaps treated as perturbations (delocalizations). The largest delocalization energies were found for the six V–O bonds between the six cage vanadiums and their terminal oxido groups. The most significant delocalization energies were observed for the 2s orbitals of O1 (Table 4).

Attempts to describe the bonding of the bridging alcoholate and oxido oxygen atoms by means of 'classical' two-centre bonds have all failed and the formalism of the 3-center 4-electron (3c4e) 'hyperbonds' had to be adopted instead. The concept of 3c4e bonding, introduced originally by Pimentel,[20] considers interactions of this type as a bonding between a triad of atoms (denoted henceforth as A1, A2, and A3), whose hybrids form three molecular orbitals (MO) of which the lowest two are populated by four electrons. Since a 3c4e interaction is usually of an $n_{A1} \rightarrow \sigma^*_{A2-A3}$ delocalization, the second populated orbital is quite high in energy. Using Coulson's description,[21] one can regard a 3c4e bond as a resonance between two limiting Lewis structures A1–A2:A3 and A1:A2–A3, denoted usually as A1⊦A2⊣A3.

Actually, the bridging oxygen atoms in the hexavanadate anion of **2** are all bonded by the 3c4e bonds (Table 5) with the vanadium atoms acting as centres for these three-centre interactions. Although the ratios between the two Lewis forms of the resonance triads are based on estimation and should be regarded as correct qualitatively,[22] the fractional bonding of the individual oxygen atoms is very well apparent.

The incorporation of σ* interactions in the second (and populated) orbitals of all the 3c4e hyperbonds leads to their energy becoming high. The oxygen nonbonding lone pairs remain also virtually nonbonding and as a consequence

Table 2 Natural charges (q_{nat}) of the hexavanadate oxygen atoms

Atom(s)	q_{nat}	Atoms	q_{nat}
O1	−1.11	O9/9′	−0.68
O2/2′, O3/3′, O7/7′	−0.74	O6/6′	−0.53
O4/4′, O5/5′	−0.69	O8/8′, O10/10′	−0.56

Table 3 Mayer bond orders (BO) for the VO_6 octahedron around V2

Bond	Mayer BO	Bond	Mayer BO
V2–O1(c)	0.634	V2–O8(t)	0.235
V2–O2(a)	0.776	V2–O9(b)	1.673
V2–O7(a)	0.686	V2–O4′(b)	1.153

Table 4 Delocalization energies (in kcal mol^{-1}) of the O1 2s orbital based on second-order perturbative estimates

Acceptor	E_{deloc} LP(2s)	Acceptor	E_{deloc} LP(2s)
V1–O6	21.97	V3–O10	23.30
V′–O6′	22.17	V3′–O10′	24.01
V2–O8, V2′–O8′	26.17	—	—

Table 5 The 3c4e hyperbonds in the hexavanadate anion[a]

Hyperbond A1⊦A2⊣A3	%A1–A2/%A2–A3	Occupancy
O3⊦V1⊣O4	37.4/62.6	3.9220
O3⊦V1⊣O5	47.1/52.9	3.9259
O4⊦V1⊣O2	60.4/39.6	3.9833
O5⊦V1⊣O3	59.3/40.7	3.9351
O2⊦V2⊣O9	39.6/60.4	3.9047
O9⊦V2⊣O7	61.1/38.9	3.9389

[a] Only contributions involving the oxygen atoms in the asymmetric part are listed.

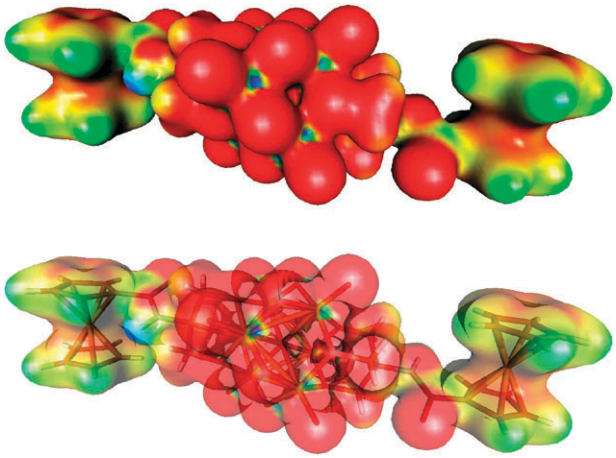

Fig. 6 Electrostatic potential mapped onto the 2% probability isosurface of **2a** (top) and orientation of the molecule in the isodensity contour (bottom). Blue regions are electrophilic, green electroneutral, and the red nucleophilic.

of both these phenomena, the highest occupied canonical orbitals delocalize over the hexavanadate cage. Due to the presence of the highly electronegative oxygen atoms, the overall electrostatic potential is also markedly negative (Fig. 6).

Since the upper 11 occupied molecular orbitals (including the HOMO) are delocalized over the hexavanadate cage, any oxidation processes will affect the anionic part of the molecule without the involvement of redox changes on the ferrocene units. The HOMO orbital particularly is a combination of the nonbonding lone pairs on the six bridging oxido atoms, each contributing with comparable fractions. The next occupied orbitals, still close in energy to the HOMO, incorporate already the bonds to the vanadium atoms. The irreversible oxidative wave observed during cyclic voltammetry (oxidation) thus probably reflects structural reorganisation at the hexavanadate cage, possibly due to changes occurring in the O–V–O triads.

Conclusions

This contribution demonstrates that the synthetic methodology developed for the synthesis of triolato-capped hexavanadates can be advantageously used for the preparation of well-defined compounds bearing the ferrocenyl groups as redox-active organometallic pendants. Electrochemical data and, mainly, theoretical computations indicate the ferrocenyl groups to behave largely as auxiliary modifiers without any pronounced electronic interaction with the anionic hexavanadate core. DFT calculations also reveal the presence of 3-centre 4-electron (3c4e) O–V–O bonds and delocalised bonding within the polyoxometalate cage where the central oxygen atom acts as an electrostatic pivot.

Experimental

Materials and methods

Syntheses were performed under argon atmosphere in the dark. Fluorocarbonylferrocene[23] and $(Bu_4N)_3[H_3V_{10}O_{28}]$[24] were synthesised according to literature procedures. Dry acetonitrile, DMF and DMA were purchased from Fluka and Aldrich. Other chemicals and solvents were used as received (Fluka, Aldrich; solvents from Lach-Ner).

NMR spectra were measured with a Varian UNITY Inova 400 spectrometer (^{1}H, 399.95; ^{13}C, 100.58; ^{51}V, 105.18 MHz) at 298 K. Chemical shifts (δ/ppm) are given relative to internal $SiMe_4$ (^{1}H and ^{13}C) or to external neat $VOCl_3$ (^{51}V). In addition to the standard notation of the signal multiplicity, vt is used to denote virtual triplets arising from magnetically non-equivalent AA′BB′ spin systems formed by the protons at the substituted cyclopentadienyl rings (C_5H_4). IR spectra were recorded with an FTIR Nicolet 7600 (Thermo Fisher Scientific) instrument in the range 400–4000 cm^{-1}. Electrospray ionisation mass spectra (ESI MS) were recorded with a Esquire 3000 (Bruker) spectrometer in methanol.

Electrochemical measurements were carried out with a computer-controlled multipurpose potentiostat μAUTOLAB III (Eco Chemie) at room temperature using a standard three-electrode cell with platinum disc electrode (AUTOLAB RDE, 3 mm diameter) as the working electrode, platinum sheet auxiliary electrode, and saturated calomel reference electrode (SCE), which was separated from the analysed solution by a salt-bridge (0.1 M Bu_4NPF_6 in MeCN). The analysed compounds were dissolved in MeCN (Aldrich, absolute) to give a solution containing *ca.* 5×10^{-4} M of the analyte and 0.1 M Bu_4NPF_6 (Fluka, puriss for electrochemistry) as the supporting electrolyte. The solutions were deaerated with argon prior to the measurement and then kept under an argon blanket. The redox potentials are given relative to the ferrocene/ferrocenium reference.

Syntheses

{*N*-[Tris(hydroxymethyl)methyl]carbamoyl}ferrocene (1). (Fluorocarbonyl)ferrocene (1.160 g, 5.0 mmol), tris(hydroxymethyl)methylamine (0.787 g, 6.5 mmol) and 4-(dimethylamino)-pyridine (0.122 g, 1.0 mmol) were dissolved in a mixture of dry DMF (20 mL) and triethylamine (1 mL), and the resulting mixture was stirred at 60 °C for 16 h. Then, the volatiles were removed under reduced pressure, and the solid residue was purified by column chromatography (silica, CH_2Cl_2–methanol, 10 : 1 v/v). Two bands were collected. The second band containing the desired product was evaporated and the residue was crystallised from hot ethyl acetate (20 mL) by slow cooling down to −18 °C. Yield of **1**·1/3AcOEt: 0.358 g (20%), orange brown crystalline solid.

^{1}H NMR (DMSO): δ 1.18 (t, $^3J_{HH}$ = 7.1 Hz, 1 H, $CH_3CO_2CH_2CH_3$), 1.99 (s, 1 H, CH_3CO_2Et), 3.64 (d, $^2J_{HH}$ = 5.7 Hz, 6 H, CH_2OH; the signal collapses into a singlet upon addition of D_2O), 4.03 (q, $^3J_{HH}$ = 7.1 Hz, 2/3 H, $CH_3CO_2CH_2CH_3$), 4.21 (s, 5 H, C_5H_5), 4.36 and 4.76 (2× virtual t, $J \approx 2.0$ Hz, 2 H, C_5H_4); 4.88 (t, $^3J_{HH}$ = 5.9 Hz, 3 H, CH_2OH; the signal disappears after the addition of D_2O), 6.63 (s, 1 H, CONH). ^{13}C{^{1}H} NMR ($CDCl_3$): δ 13.98 ($CH_3CO_2CH_2CH_3$), 20.65 (CH_3CO_2Et), 59.64 ($CH_3CO_2CH_2CH_3$), 60.58 (CH_2OH), 62.06 (CNH), 68.19 (CH of C_5H_4), 69.49 (C_5H_5), 70.03 (CH of C_5H_4), 76.56 (C_{ipso} of C_5H_4), 170.10 (C=O; only one C=O resonance

was observed). IR (neat): ν/cm^{-1} 3260 br s, 3108 m, 2959 m, 2938 m, 2896 w, 2872 w, 1740 s, 1619 vs, 1535 s, 1459 w, 1449 w, 1412 w, 1375 m, 1344 m, 1307 m, 1286 w, 1240 m, 1190 m, 1122 m, 1106 w, 1074 w, 1054 s, 1036 m, 1020 s, 930 w, 906 w, 872 w, 847 w, 831 m, 773 m, 730 br m, 620 w, 584 w, 560 w, 529 m, 499 m, 484 m, 467 w cm^{-1}. Anal. Calc. for $C_{15}H_{19}FeNO_4 \cdot 1/3CH_3CO_2Et$ (359.6): C 54.11, H 6.00, N 3.90%. Found: C 53.74, H 5.97, N 3.75%.

Compound 2. A solution of amide **1b** (0.321 g, 0.9 mmol) and $(Bu_4N)_3[H_3V_{10}O_{28}]$ (0.502 g, 0.3 mmol) in dry DMA (10 mL) was heated at 90 °C for 60 h, whereupon the colour turned from orange to brown. The reaction mixture was cooled to room temperature and then slowly added to diethyl ether (100 mL). The separated brown precipitate was filtered off and purified by column chromatography (silica gel, MeCN). The first brown and green coloured bands were discarded, and the following red band was collected and evaporated under vacuum. The solid residue, which was shown to be essentially pure *unsolvated* **2** by NMR spectra, was dissolved in dry DMF (2 mL). The solution was carefully layered with MeCN (1 mL) and diethyl ether (20 mL), and the mixture was allowed to crystallise over several days to afford crystalline **2a**, which was isolated by suction. The isolated product was recrystallised once again to afford analytically pure **2a** as a dark red crystalline solid. Yield: 81 mg (15%).

^{1}H NMR (CD_3CN): δ 0.98 (br t, 12 H, $NCH_2(CH_2)_2CH_3$), 1.38 and 1.63 (2× br s, 8 H, $NCH_2(CH_2)_2CH_3$); 2.78 and 2.90 (2× s, 3 H, Me_2NCHO); 3.14 (br s, 8 H, $NCH_2(CH_2)_2CH_3$), 4.16 (s, 5 H, C_5H_5), 4.32 and 4.71 (2× virtual t, J = 1.9 Hz, 2 H, C_5H_4); 5.37 (s, 6 H, $NHC(CH_2O)_3$), 5.77 (s, 1 H, $NHC(CH_2O)_3$), 7.95 (br s, 1 H, Me_2NCHO). $^{13}C\{^1H\}$ NMR (CD_3CN): δ 13.94 ($NCH_2(CH_2)_2CH_3$), 20.45 and 24.47 ($NCH_2(CH_2)_2CH_3$); 31.34 and 36.62 (Me_2NCHO); 54.26 (*C*NH), 59.44 (t(1 : 1 : 1), $^1J(^{14}N,^{13}C) \approx 3$ Hz, $NCH_2(CH_2)_2CH_3$), 69.52 (*C*H of C_5H_4), 70.80 (C_5H_5), 71.35 (*C*H of C_5H_4), 77.61 (C_{ipso} of C_5H_4), 83.88 (CH_2O), 170.90 (Fc*C*O); the C=O signal due to Me_2NCHO was not observed. ^{51}V NMR (CD_3CN): δ −498 (br s, $\Delta\nu_{\frac{1}{2}} \approx 530$ Hz). ESI± MS (CH_3OH): m/z 242 (Bu_4N^+); 587 ($[\{FcCONHC(CH_2O)_3\}_2V_6O_{13}]^{2-}$) and 1197 ($[\{FcCONHC(CH_2O)_3\}_2V_6O_{13} + Na]^-$). IR (neat): ν/cm^{-1} 3337 m, 3308 m, 3101 w, 3084 w, 2962 m, 2938 m, 2873 m, 2856 m, 1674 s, 1655/1652 s, 1536/1533 s, 1471 m, 1410 w, 1386 m, 1312 m, 1275 m, 1195 w, 1170 w, 1106 s, 1060 m, 1047 m, 1020 w, 952 vs, 817/810 s, 722 s, 584 s, 497 w, 481 w, 422 m. Anal. Calc. for $(C_{16}H_{36}N)_2[C_{30}H_{32}Fe_2N_2O_{21}V_6] \cdot 2C_3H_7NO$ (1805.0): C 45.24, H 6.59, N 4.66%. Found: C 44.92, H 6.51, N 4.55%.

X-Ray crystallography

Single crystals suitable for X-ray diffraction measurements were grown from warm ethyl acetate (**1**·1/2CH_3CO_2Et: brown plate, 0.20 × 0.32 × 0.40 mm^3) or selected directly from the reaction batch (**2a**: red-brown fragment, 0.20 × 0.25 × 0.28 mm^3). The selected specimens were mounted onto glass fibres with poly(perfluoroalkylether) oil.

Full-set diffraction data ($2\theta \leq 54.9$ for **1**, and 52.8° for **2a**; $\pm h \pm k \pm l$, data completeness 99.9%) were collected with a Nonius KappaCCD diffractometer equipped with a Cryostream Cooler (Oxford Cryosystems) using graphite-monochromatised MoKα radiation (λ = 0.71073 Å). The data were analysed with the HKL program package;[25] absorption was neglected.

Table 6 Selected crystallographic data and structure refinement parameters for **1a** and **2a**[a]

Compound	**1a**	**2a**
Formula	$C_{17}H_{23}FeNO_5$[e]	$C_{68}H_{118}Fe_2N_6O_{23}V_6$[f]
M	377.21	1805.02
Crystal system	Monoclinic	Triclinic
Space group	$C2/c$ (no. 15)	$P\bar{1}$ (no. 2)
a/Å	29.2486(4)	12.6480(2)
b/Å	10.1996(1)	15.8602(2)
c/Å	11.8137(1)	20.3923(3)
α/°	—	84.8847(8)
β/°	103.1641(9)	79.9909(7)
γ/°	—	78.0411(8)
V/Å^3	3431.70(8)	3935.0(1)
Z	8	2
D_c/g mL^{-1}	1.460	1.523
μ(MoKα)/mm^{-1}	0.905	1.113
Diffractions collected	45736	105274
Independent/observed[b] diffrns	3930/3622	16120/12513
R_{int}[c] (%)	2.9	5.8
R[d] observed diffractions (%)	3.02	4.25
R, wR[d] all data (%)	3.30, 7.91	6.20, 11.3
$\Delta\rho$/e Å^{-3}	0.58, −0.52	0.82, −0.55
CCDC reference number	779152	779153

[a] Common details: T = 150(2) K. [b] Diffractions with $I > 2\sigma(I)$. [c] $R_{int} = \sum|F_o^2 - F_o^2(\text{mean})|/\sum F_o^2$, where F_o^2(mean) is the average intensity of symmetry-equivalent diffractions. [d] $R_1 = \sum||F_o| - |F_c||/\sum|F_o|$, $wR = [\sum\{w(F_o^2 - F_c^2)^2\}/\Sigma w(F_o^2)^2]^{\frac{1}{2}}$. [e] $C_{15}H_{19}FeNO_4 \cdot 1/2C_4H_8O_2$. [f] $(C_{16}H_{36}N)_2[C_{30}H_{32}Fe_2N_2O_{21}V_6] \cdot 2C_3H_7NO$.

The phase problems were solved by direct methods (SIR97)[26] and the structures were refined by full-matrix least-squares on F^2 (SHELXL-97).[27] The non-hydrogen atoms were refined with anisotropic displacement parameters except for disordered ethyl acetate in the structure of amide **1**. The NH and OH hydrogens were located on difference electron density maps and refined as riding atoms with U_{iso}(H) assigned to a multiple of U_{eq} of their bonding atom. All other hydrogen atoms were included in their theoretical positions and refined as riding atoms.

Geometric calculations were performed with a recent version of the PLATON program.[12] All numerical values are rounded with respect to their estimated standard deviations (esd's) given with one decimal; parameters involving fixed hydrogen atoms are given without esd's. Relevant crystallographic data and structure refinement parameters are presented in Table 6.

Theoretical calculations

DFT computations have been conducted at the *fermi* cluster of the Computer Centre at the J. Heyrovský Institute of Physical Chemistry, Academy of Sciences of the Czech Republic, using Gaussian 03, Revision E.01.[28] The calculations were carried out as single point on the solid state geometry with the cationic parts excluded. The B3P86 functional was employed and the 6-31+G(d) basis set was used for all atoms. Natural Bond Orbital Analyses were done with the NBO 5.G[29] program;

visualization of the canonical molecular orbitals and the overall electrostatic potential was accomplished by Molden.[30]

Acknowledgements

This work was financially supported by the Grant Agency of Charles University in Prague (project no. 69309) and is a part of long-term research projects of Faculty of Science, Charles University in Prague, supported by the Ministry of Education, Youth and Sports of the Czech Republic (projects nos. MSM0021620857 and LC06070).

Notes and references

1 (*a*) M. T. Pope, *Heteropoly and Isopoly Oxometalates*, Springer, Berlin, 1983; (*b*) M. T. Pope, *Isopolyanions and Heteropolyanions*, in *Comprehensive Coordination Chemistry II*, ed. J. A. McCleverty and T. B. Mayer, Elsevier, Amsterdam, **2004**, vol. 4, ch. 4.10, p. 635; (*c*) C. M. Hill, *Polyoxo Anions: Reactivity*, in *Comprehensive Coordination Chemistry II*, ed. J. A. McCleverty and T. B. Mayer, Elsevier, Amsterdam, 2004, vol. 4, ch. 4.11, p. 679; (*d*) J. Zubieta, *Solid State Methods, Hydrothermal*, in *Comprehensive Coordination Chemistry II*, ed. J. A. McCleverty and T. J. Meyer, Elsevier, Amsterdam, 2004, vol. 1, ch. 1.39, p. 697.
2 (*a*) See the special issue of *Chem. Rev.* published in 1998: C. L. Hill, *Chem. Rev.*, 1998, **98**, 1; (*b*) D.-L. Long, E. Burkholder and L. Cronin, *Chem. Soc. Rev.*, 2007, **36**, 105.
3 (*a*) Y. Hayashi, Y. Ozawa and K. Isobe, *Chem. Lett.*, 1989, 425; (*b*) Y. Hayashi, Y. Ozawa and K. Isobe, *Inorg. Chem.*, 1991, **30**, 1025; (*c*) H. K. Chae, W. G. Klemperer and V. W. Day, *Inorg. Chem.*, 1989, **28**, 1423; (*d*) G. Süss-Fink, L. Plasseraud, V. Ferrand, S. Stanislas, A. Neels, H. Stoeckli-Evans, M. Henry, G. Laurenczy and R. Roulet, *Polyhedron*, 1998, **17**, 2817.
4 For representative examples, see: (*a*) D. Hou, G.-S. Kim, K. S. Hagen and C. L. Hill, *Inorg. Chim. Acta*, 1993, **211**, 127; (*b*) J. Spandl, C. Daniel, I. Brudga and H. Hartl, *Angew. Chem., Int. Ed.*, 2003, **42**, 1163; (*c*) C. Daniel and H. Hartl, *J. Am. Chem. Soc.*, 2005, **127**, 13978; (*d*) M. A. Augustyniak-Jablokow, C. Daniel, H. Hartl, J. Spandl and Y. V. Yablokov, *Inorg. Chem.*, 2008, **47**, 322.
5 (*a*) Q. Chen and J. Zubieta, *Inorg. Chem.*, 1990, **29**, 1456; (*b*) M. I. Khan, Q. Chen, J. Zubieta and D. P. Goshorn, *Inorg. Chem.*, 1992, **31**, 1556; (*c*) Q. Chen and J. Zubieta, *Inorg. Chim. Acta*, 1992, **198–200**, 95; (*d*) Q. Chen, D. P. Goshorn, C. P. Scholes, X. Tan and J. Zubieta, *J. Am. Chem. Soc.*, 1992, **114**, 4667; (*e*) Q. Chen and J. Zubieta, *Chem. Commun.*, 1993, 1180; (*f*) M. I. Khan, Q. Chen, H. Hope, S. Parkin, C. J. O'Connor and J. Zubieta, *Inorg. Chem.*, 1993, **32**, 2929; (*g*) A. Müller, J. Meyer, H. Bögge, A. Stammler and A. Botar, *Z. Anorg. Allg. Chem.*, 1995, **621**, 1818.
6 (*a*) J. W. Han, K. I. Hardcastle and C. L. Hill, *Eur. J. Inorg. Chem.*, 2006, 2598; (*b*) C. L. Hill, T. M. Anderson, J. W. Han, D. A. Hillesheim, Y. V. Geletii, N. M. Okun, R. Cao, B. Botar, D. G. Musaev and K. Morokuma, *J. Mol. Catal. A: Chem.*, 2006, **251**, 234; (*c*) J. W. Han and C. L. Hill, *J. Am. Chem. Soc.*, 2007, **129**, 15094.
7 R. M. Silverstein, F. X. Webster and D. J. Kiemle, *Spectrometric Identification of Organic Compounds*, Wiley, New York, 7th edn, 2005, ch. 2, p. 99.
8 P. Štěpnička and I. Císařová, *CrystEngComm*, 2005, **7**, 37.
9 L. Lin, A. Berces and H.-B. Kraatz, *J. Organomet. Chem.*, 1998, **556**, 11.
10 M. Oberhoff, L. Duda, J. Karl, E. Mohr, G. Erker, R. Fröhlich and M. Grehl, *Organometallics*, 1996, **15**, 4005.
11 M. B. Hursthouse, S. J. Coles and J. H. R. Tucker, private communication to the Cambridge Crystallographic Data Centre (refcode: BATLEO).
12 (*a*) A. L. Spek, *J. Appl. Crystallogr.*, 2003, **36**, 7; (*b*) The program is available *via* the Internet at http://xray5.chem.uu.nl/spek/platon/.
13 Another potential intramoleculear N–H1N···O4 contact has a rather unfavourable geometry: N–H1N···O4, N···O4 = 2.789(2) Å, angle at H1N = 107°.
14 Molecular structures of the crystallographically independent anions differ by the orientation of the C(O)NH unit (*i.e.*, O and NH interchange their positions) to the vanadate core (see ESI†, Fig. S2).
15 Values in the square brackets refer to cation 2.
16 For both structurally independent cations, the N–C distances and C–N–C angles fall into the ranges of 1.503(2)–1.528(2) Å and 105.2(2)–111.7(2)°, respectively. For the DMF molecules, the C═O and C–N distances are 1.191(6)/1.188(6) and 1.330(6)/1.316(6) Å, respectively (molecule 1/molecule 2). The respective N–C–O angles are 125.7(5)/126.5(5)°.
17 C. Hansch, A. Leo and R. W. Taft, *Chem. Rev.*, 1991, **91**, 165.
18 (*a*) I. Mayer, *Chem. Phys. Lett.*, 1983, **97**, 270; (*b*) I. Mayer, *Int. J. Quantum Chem.*, 1984, **26**, 151.
19 J. P. Foster and F. Weinhold, *J. Am. Chem. Soc.*, 1980, **102**, 7211.
20 G. C. Pimentel, *J. Chem. Phys.*, 1951, **19**, 446.
21 C. A. Coulson, *J. Chem. Soc.*, 1964, 1442.
22 F. Weinhold and C. R. Landis, *Valency and Bonding: A Natural Bond Orbital Donor-Acceptor Perspective*, Cambridge University Press, Cambridge, UK, 2005.
23 T. H. Galow, J. Rodrigo, K. Cleary, G. Cooke and V. M. Rotello, *J. Org. Chem.*, 1999, **64**, 3745.
24 V. W. Day, W. G. Klemper and D. J. Maltbie, *J. Am. Chem. Soc.*, 1987, **109**, 2991.
25 Z. Otwinowski and W. Minor, *Methods Enzymol.*, 1997, **276**, 307.
26 A. Altomare, M. C. Burla, M. Camalli, G. L. Cascarano, C. Giacovazzo, A. Guagliardi, A. G. G. Moliterni, G. Polidori and R. Spagna, *J. Appl. Crystallogr.*, 1999, **32**, 115.
27 (*a*) G. M. Sheldrick, *Acta Crystallogr., Sect. A: Found. Crystallogr.*, 2008, **64**, 112; (*b*) The program is available *via* the Internet at http://shelx.uni-ac.gwdg.de/SHELX/.
28 M. J. Frisch, G. W. Trucks, H. B. Schlegel, G. E. Scuseria, M. A. Robb, J. R. Cheeseman, J. A. Montgomery, Jr., T. Vreven, K. N. Kudin, J. C. Burant, J. M. Millam, S. S. Iyengar, J. Tomasi, V. Barone, B. Mennucci, M. Cossi, G. Scalmani, N. Rega, G. A. Petersson, H. Nakatsuji, M. Hada, M. Ehara, K. Toyota, R. Fukuda, J. Hasegawa, M. Ishida, T. Nakajima, Y. Honda, O. Kitao, H. Nakai, M. Klene, X. Li, J. E. Knox, H. P. Hratchian, J. B. Cross, V. Bakken, C. Adamo, J. Jaramillo, R. Gomperts, R. E. Stratmann, O. Yazyev, A. J. Austin, R. Cammi, C. Pomelli, J. W. Ochterski, P. Y. Ayala, K. Morokuma, G. A. Voth, P. Salvador, J. J. Dannenberg, V. G. Zakrzewski, S. Dapprich, A. D. Daniels, M. C. Strain, Ö. Farkas, D. K. Malick, A. D. Rabuck, K. Raghavachari, J. B. Foresman, J. V. Ortiz, Q. Cui, A. G. Baboul, S. Clifford, J. Cioslowski, B. B. Stefanov, G. Liu, A. Liashenko, P. Piskorz, I. Komaromi, R. L. Martin, D. J. Fox, T. Keith, M. A. Al-Laham, C. Y. Peng, A. Nanayakkara, M. Challacombe, P. M. W. Gill, B. Johnson, W. Chen, M. W. Wong, C. Gonzalez and J. A. Pople, *Gaussian 03, Revision E.01*, Gaussian, Inc., Wallingford CT, USA, 2004.
29 E. D. Glendening, J. Badenhoop, A. E. Reed, J. E. Carpenter, J. A. Bohmann, C. M. Morales and F. Weinhold, *Theoretical Chemistry Institute*, University of Wisconsin, Madison, USA, 2001.
30 G. Schaftenaar and J. H. Noordik, *J. Comput.-Aided Mol. Des.*, 2000, **14**, 123.

